REGULAR ARTICLE

Polymer Journal

Special Issues –International Symposium on Polymer Crystallization 2007–

Crystallization after Orientation Relaxation in Polypropylene

*By Kayo HASHIMOTO and Hiromu SAITO**

We investigated the isothermal crystallization of polypropylene after the relaxation of shear orientation by using a digital polarized microscope and Hv light scattering. Small spherulites with diffuse Maltese cross extinction patterns are obtained by crystallization after orientation relaxation while large mixed spherulites with no Maltese cross patterns are obtained by crystallization under quiescent conditions, suggesting the suppression of subsidiary lamellae by crystallization after the orientation relaxation. The Hv light scattering intensity increased gradually during the radial growth and then steeply in spite of the cessation of the radial growth of the spherulites. A theoretical analysis of the scattering profile, based on random orientation approximation, revealed that the size of the domain consisting of lamellae arranged in parallel increases in the spherulite in spite of the cessation of the radial growth of the spherulite. Such characteristic crystallization behavior might be attributed to the locally oriented chains that remain after orientation relaxation.

KEY WORDS: Crystallization / Morphology / Orientation Relaxation / Polypropylene / Light Scattering / Microscope /

It is well known that spherulites of isotactic polypropylene (PP) consist of crosshatched lamellar branching. That is, subsidiary lamellae grow tangentially to the radiating primary lamellae.[1–8] Because of the crosshatched lamellae, mixed spherulites consisting of fibrils with positive and negative birefringence are obtained. The crosshatched structure is formed by epitaxial crystallization of the subsidiary lamellae on the lateral (010) face of the radiating primary lamellae.[9–13]

In order to control the crystalline morphology of PP, elongation-induced crystallization is of great interest. Due to the elongation, polymer chains are oriented in the melt and the crystalline morphologies are different from those obtained under quiescent conditions. Spherulites are obtained by crystallization under quiescent conditions, whereas "shish-kebabs,"[14,15] row-structure,[16] skin-core morphology,[17] and so on are obtained under shear orientation.[18] The applied shear elongation immediately produces bundles of parallel chain fragments, forming primary nuclei like shish. Nucleation then occurs from the primary nuclei caused by diffusion of new chain segments from the relaxed melt, and folded chain lamellae grow as kebabs in the lateral direction of the shish.[14] In contrast, the melt history of crystalline polymers affects the crystallization behavior, that is, a melt-memory effect.[19,20] The nucleation rate of the crystallites depends on the melt temperature, *e.g.*, the nucleation rate of crystallization after melting is fast when the crystallized specimen is melted just above the melting temperature due to the residual crystalline nuclei.

It is well known that polymer in the melting state is random coil. When the polymer is elongated, the polymer chain is oriented. With time, the oriented chain is relaxed to the random coil state. However, locally stretched chains with parallel alignment might remain although the oriented chain is completely relaxed on a macroscopic scale. Because the locally oriented chains remain after orientation relaxation, the crystallization after orientation relaxation is expected to be different from that of the quiescent conditions. In this paper, to confirm the influence of locally oriented chains on crystallization behavior, we investigate the isothermal crystallization of polypropylene after the orientation relaxation of shear elongation by using Hv light scattering and a high-fidelity digital microscope. The crystalline morphologies thus obtained are discussed by the results obtained from a polarized optical microscope and differential scanning calorimetry (DSC).

EXPERIMENTAL

The PP specimen used in this study was supplied by Japan Polychem Corporation ($M_w = 3.0 \times 10^5$). The PP powder was compression molded between metal plates at 190 °C for 5 min and then quickly quenched in a water bath to obtain a film specimen with a thickness of about 80 μm.

In order to perform *in situ* observation of the crystallization growth under a variety of shear conditions, we designed a special heat-drawing apparatus (Far-East Manufacturing Inc.), as shown in Figure 1. Two optical glass windows were mounted on the apparatus. The diameter of the bottom window is 10 mm, which allows a He-Ne laser beam or white light to irradiate the specimen, and the diameter of the upper window is 40 mm, which allows scattered light to pass. The film specimen (10 mm × 10 mm) was put between two parallel glass plates, which were fixed by clamps, and held at 190 °C for 5 min to melt the crystallites and ensure strong adhesion between the glass plates and the film specimen. After the specimen melted, the step shear was applied to the film specimen by translating both slide glasses at a constant shear rate of $10^4\ s^{-1}$ at 190 °C. Subsequently, the specimen was gradually cooled at a rate of 3.5 °C/min to the crystallization temperature $T_c = 140$ °C. The development of the PP spherulites during the isothermal annealing at the T_c was observed under a high-fidelity digital microscope (MX-5030 SZII; Hirox Co., Ltd.) equipped with

Department of Organic and Polymer Materials Chemistry, Tokyo University of Agriculture and Technology, Koganei 184-8588, Japan
*To whom correspondence should be addressed (Tel/Fax: +81-42-388-7294; E-mail: hsaitou@cc.tuat.ac.jp).

 doi:10.1295/polymj.PJ2007187

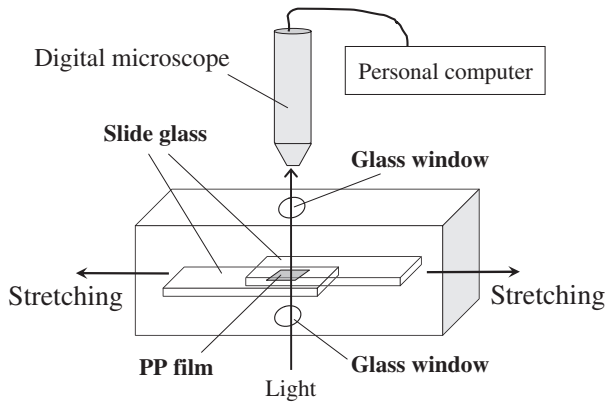

Figure 1. Schematic illustration of heat-drawing apparatus equipped with digital high-fidelity microscope.

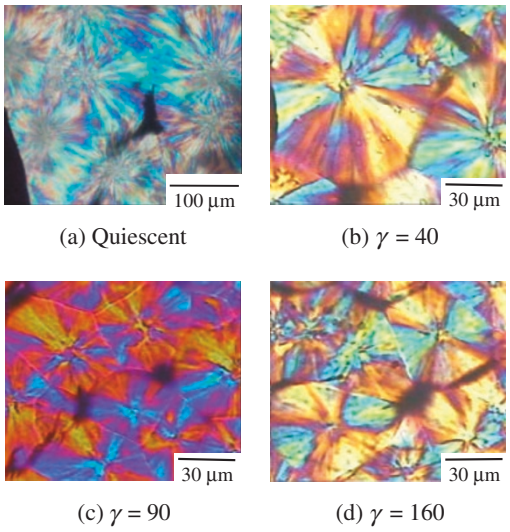

Figure 2. Polarized optical micrographs of PP crystallized at $T_c = 140\,^{\circ}C$ after shear orientation at 190 °C.

the above heat-drawing apparatus. For a clear image of the structure, halogen light was irradiated through the specimen from the bottom window of the apparatus. This microscopic system provides real-time observation of the structure with a resolution of several micrometers. Information from the digital high-fidelity microscope was recorded on a personal computer using an image capture board and imaging software.

Real-time analysis of the isothermal crystallization was also performed by a light scattering apparatus. A polarized He-Ne laser of wavelength 632.8 nm was applied vertically to the film specimen in the heat-drawing apparatus described above. The scattered light passed through an analyzer and then onto a highly sensitive charge-coupled device (CCD) camera with a 512×512 pixel sensor having dimensions of $13.3\,mm \times 8.8\,mm$ (Princeton Instruments, Inc., TE/CDD-512-TKM-1). We employed H_v geometry in which the optical axis of the analyzer was set perpendicular to that of the polarizer. This sensor provides time-resolved measurements of a two-dimensional angular distribution of scattered light with 512 one-dimensional data points in a time scale of 0.2 s. The input data from the CCD camera was digitized by an ST-13X controller and then stored in a personal computer for further analysis.[21]

The crystallized PP specimen thus obtained was cooled to room temperature. Then, the crystalline morphology of the specimen was observed with a polarized optical microscope (BX-50, Olympus Co., Ltd.). Measurement by a DSC was carried out using a Perkin Elmer Pyris 1 DSC at a heating rate of $10\,^{\circ}C\,min^{-1}$ in an atmosphere of N_2.

RESULTS AND DISCUSSION

Figure 2 shows polarized optical micrographs of PP crystallized at $T_c = 140\,^{\circ}C$ under quiescent condition (qui-PP) and after orientation relaxation for various shear strains γ (rel-PP). A large spherulite having a radius of 80 μm is seen in the qui-PP (Figure 2a). The Maltese cross extinction pattern is unclear, and fibrils with a different contrast radiate from the center of the spherulite. The different contrast is attributed to the different signs of birefringence, that is, fibrils with different colors are observed under a sensitive tint plate, indicating that both positive and negative birefringent fibrils are mixed in the spherulite. This type of spherulite is called a "mixed spherulite." A mixed spherulite consists of crosshatched lamellae in which subsidiary lamellae grow tangentially to the primary radiating lamellae.[1–9]

The radius of the spherulites becomes smaller by orientation relaxation before crystallization, *i.e.*, the radius is 55 μm at the shear strain of $\gamma = 40$ (Figure 2b), 30 μm at $\gamma = 90$ (Figure 2c), and 25 μm at $\gamma = 160$ (Figure 2d), while the radius is 80 μm in the qui-PP (Figure 2a). This might imply that the rate of nucleation increases by orientation relaxation before crystallization. The interesting result here is that a diffuse Maltese cross extinction pattern is observed in the rel-PP. The Maltese cross extinction pattern becomes clearer and the birefringence in the spherulite becomes larger with an increased γ, suggesting that the ordering in the spherulite becomes larger with an increased γ. This might be caused by the suppression of subsidiary lamellae growth tangential to the primary radiating lamellae. The increase of the nucleation rate and the suppression of the subsidiary lamellae might be attributed to the locally oriented chains that remain after the orientation relaxation.

Figure 3 shows the *in situ* observation of the spherulite growth during the melt crystallization of the qui-PP and the rel-PP at 140 °C. Due to the orientation relaxation on a macroscopic scale, the shape of the spherulite is spherical during overall crystallization. The spherulites grow with time and their radial growth stops at around 8 min by truncation of the spherulites. The nucleation density of the rel-PP is higher than that of the qui-PP, suggesting that the rate of nucleation of the rel-PP is faster than that of the qui-PP. This result is consistent with the small spherulite of the rel-PP shown in Figure 2. In order to better understand the characteristic crystallization behavior of the rel-PP, the light scattering results are demonstrated in the following paragraphs.

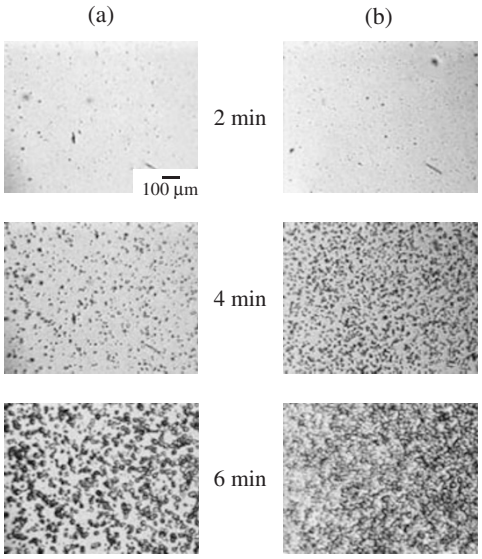

Figure 3. Optical micrographs of the spherical growth of PP crystallized at $T_c = 140\,^{\circ}C$: (a) at quiescent condition, (b) after shear orientation at 190 °C.

The Hv light scattering patterns from the qui-PP and the rel-PP were circularly symmetric, *i.e.*, there was no azimuthal angular dependence. This suggests that the optical axes of the crystals are randomly oriented in the spherulites. In this case, to discuss the kinetic aspect of the crystallization, it is convenient to employ the integrated scattering intensity in Hv mode, *i.e.*, the invariant Q_{Hv} defined by:[21,22]

$$Q_{Hv} = \int_0^\infty I(q) q^2 dq \tag{1}$$

where $I(q)$ is the intensity of the scattered light at the scattering vector q; $q = (4\pi/\lambda)/\sin(\theta/2)$, λ and θ being the wavelength of the light and the scattering angle, respectively. Q_{Hv} is described by the mean square optical anisotropy δ:

$$Q_{Hv} \propto \langle \delta^2 \rangle = \phi_S (\alpha_r - \alpha_t)^2 \tag{2}$$

where ϕ_S is the volume fraction of the spherulite, and α_r and α_t are the radial and tangential polarizabilities of the spherulites, respectively. Hence, Q_{Hv} is expected to increase with an increasing volume fraction of the spherulites and the $(\alpha_r - \alpha_t)$ associated with ordering in the spherulites.

The time variation of invariants Q_{Hv} for the qui-PP and the rel-PP ($\gamma = 125$) are shown in Figure 4. Q_{Hv} of the qui-PP increases with time and levels off at $t = 9$ min, as expected from eq 2 when $(\alpha_r - \alpha_t)$ is constant during crystallization, *i.e.*, ϕ_S increases and attains its maximum value when the spherulites fill the whole space. In contrast, Q_{Hv} of the rel-PP increases gradually with time, and then increases steeply after $t = 8$ min, at which point the radial growth of the spherulites stops, and finally it levels off at $t = 15$ min. These results suggest a two-step process of crystallization growth in the rel-PP in spite of the stop of the radial growth of the spherulite while a single-step occurs in the qui-PP.

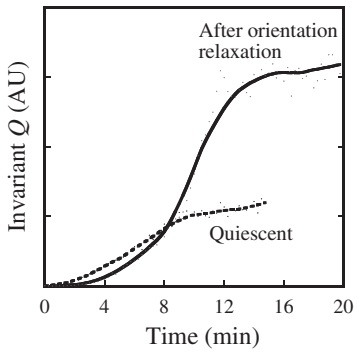

Figure 4. Time variation of invariants Q_{Hv} during isothermal crystallization at $T_c = 140\,^{\circ}C$ for quiescent condition and after shear orientation at 190 °C.

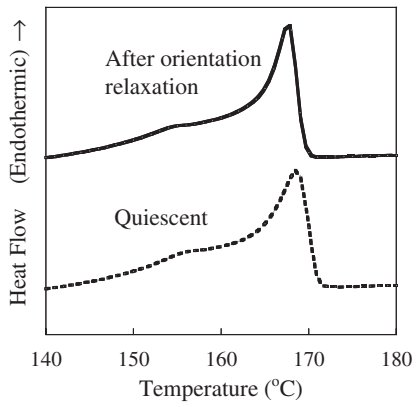

Figure 5. DSC thermograms of PP crystallized at $T_c = 140\,^{\circ}C$ for quiescent condition and after shear orientation at 190 °C.

As demonstrated in Figure 4, the maximum value of Q_{Hv} for the rel-PP is much larger than that for the qui-PP. Since Q_{Hv} is related to the difference in polarizability $(\alpha_r - \alpha_t)$, $(\alpha_r - \alpha_t)$ is ascribed to the crystallinity in the spherulite and the orientation function for the optical axis of the crystalline region. As shown in Figure 5, the area of the endothermic melting peak of the rel-PP was almost the same as that of the qui-PP, suggesting that the degree of crystallinity in the rel-PP is almost same as that in the qui-PP. Thus, the large value of Q_{Hv} for the rel-PP is caused by the high degree of orientation of the crystalline region in the spherulite. This suggests that the orientational ordering in the spherulite of the rel-PP is much larger than that of the qui-PP.

As previously demonstrated, the Hv light scattering patterns of the qui-PP and the rel-PP were circular and symmetric. In this case, the light scattering intensity I_{Hv} is described by an assumption of random orientation:[23]

$$I_{Hv} \propto \langle \delta \rangle^2 \int_0^\infty f(r) \frac{\sin qr}{qr} 4\pi r^2 dr \tag{3}$$

where $f(r)$ is the correlation function of orientation fluctuation in an optical axis at separation distance r. Assuming that $f(r)$ is given by the exponential correlation function:

$$f(r) = \exp(-r/a) \tag{4}$$

Polymer Journal

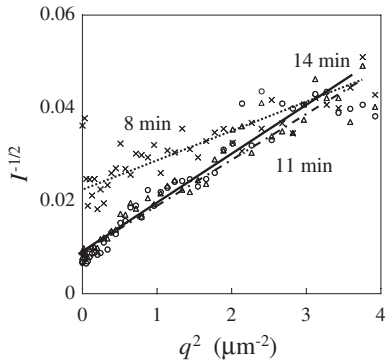

Figure 6. Debye-Bueche plots of Hv scattering intensity for PP crystallized at T_c = 140 °C after shear orientation at 190 °C.

where a is the orientation correlation distance, the angular dependence of I_{Hv} is described by the Debye-Bueche scattering function:[22–27]

$$I(q)^{-1/2} = \frac{1}{A} + \frac{a^2}{A} q^2 \tag{5}$$

where A is constant and a is the orientation correlation distance. The orientation correlation distance a is described by[26]

$$a = \frac{2d}{3\varepsilon^2} \tag{6}$$

where d is the size of lamellar stack. ε is the average angle between the optical axes of neighboring lamellar stacks and is a parameter describing the degree of disorder for the arrangement of lamellar stacks.[27,28] Hence, we can employ the orientation correlation distance a as a measure of ordering in the spherulite.

As shown in Figure 6, the plot of $I_{Hv}{}^{-1/2}$ *vs.* q^2 yielded straight lines, as expected from eq 6. The orientation correlation distance a can be obtained from the slope and the intercept in the plots of $I_{Hv}{}^{-1/2}$ *vs.* q^2. The time variation of the a in the qui-PP and in the rel-PP are shown in Figure 7. The time variation of the invariant Q_{Hv} is also shown in Figure 7. The a of the qui-PP is almost constant with time (Figure 7a). In contrast, the a of the rel-PP increases with time (Figure 7b). The a of the rel-PP starts to increase at the same time that Q_{Hv} starts to increase steeply after its gradual increase and the stop of the radial growth of the spherulite at around 8 min. Thus, the two-step increase of Q_{Hv} in the rel-PP, shown in Figure 4, might result from the increase of the a in spite of the cessation of the radial growth of the spherulites.

The results demonstrated above suggest the increase of the ordering in the spherulite during the crystallization of PP by crystallization after the orientation relaxation, as schematically shown in Figure 8. The ordering in the spherulite increases by increasing the stacks of the oriented lamellae in spite of the cessation of the radial growth of the spherulites. The increase of the oriented lamellar stacks might be enhanced by the locally oriented chains that remain after the orientation relaxation. The growth of the oriented lamellar stacks might

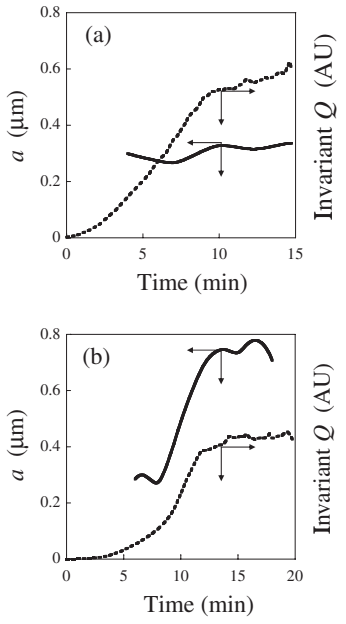

Figure 7. Time variation of orientation correlation distance a and invariant Q_{Hv}: (a) at quiescent condition, (b) after shear orientation at 190 °C.

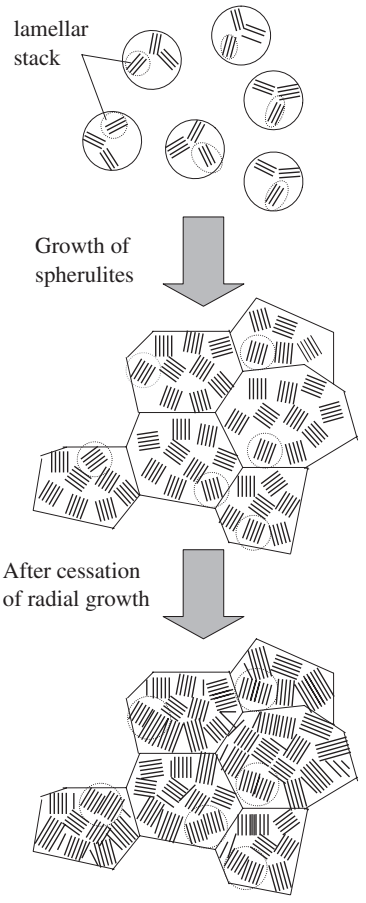

Figure 8. Schematic illustration of the crystallization behavior of PP after the orientation relaxation.

be ascribed to the suppression of the subsidiary lamellae grown tangentially to the primary radiating lamellae; this may cause the diffuse Maltese cross extinction pattern shown in Figure 2b–2d.

CONCLUSION

Small spherulites with diffuse Maltese cross extinction patterns are obtained by crystallization after the orientation relaxation of polypropylene, while mixed spherulites are obtained by crystallization in the quiescent condition. *In situ* observation and time resolved measurements of Hv light scattering revealed that the ordering in the spherulites increases in spite of the cessation of the radial growth of the spherulites by crystallization after the orientation relaxation. Such characteristic crystallization behavior might be attributed to the locally oriented chains that remain after the orientation relaxation.

Received: October 25, 2007
Accepted: April 24, 2008
Published: June 18, 2008

REFERENCES

1. E. P. Moore, Jr., "Polypropylene Handbook," Hanser/Gardner, Cincinnati, OH, 1996.
2. F. J. Padden and H. D. Keith, *J. Appl. Phys.*, **30**, 1479 (1959).
3. F. Khoury, *J. Res. Natl. Bur. Stand.*, **70A**, 2900 (1966).
4. B. R. Norton and A. Keller, *Polymer*, **26**, 704 (1985).
5. H. Awaya, *Polymer*, **29**, 591 (1988).
6. R. H. Olley and D. C. Bassett, *Polymer*, **30**, 399 (1989).
7. J. J. Janmak, S. Z. D. Cheng, P. A. Giusti, and E. T. Hsieh, *Macromolecules*, **24**, 2253 (1991).
8. J. Varga, *J. Matter. Sci.*, **27**, 2557 (1992).
9. F. J. Padden and H. D. Keith, *J. Appl. Phys.*, **37**, 4013 (1966).
10. F. L. Binsbergen and B. G. M. De Lange, *Polymer*, **9**, 23 (1968).
11. B. Lotz and J. C. Wittmann, *J. Polym. Sci., Part B: Polym. Phys.*, **24**, 1541 (1986).
12. W. Stocker, S. N. Magonov, H. J. Cantow, J. C. Wittmann, and B. Lotz, *Macromolecules*, **26**, 5915 (1993).
13. B. Lotz, J. C. Wittmann, and A. J. Lovinger, *Polymer*, **37**, 4979 (1996).
14. R. H. Somani, L. Yang, B. S. Hsiao, P. K. Agarwal, H. A. Fruitwala, and A. H. Tsou, *Macromolecules*, **35**, 9096 (2002).
15. A. Keller and M. J. Machin, *J. Macromol. Sci., Phys.*, **B1**, 41 (1967).
16. R. H. Somani, B. S. Hsiao, A. Nogales, S. Srinivas, A. H. Tsou, I. Sics, F. J. Balta-Calleja, and T. A. Ezquerra, *Macromolecules*, **33**, 9385 (2000).
17. G. Kumaraswamy, A. M. Issaian, and J. A. Kornfield, *Macromolecules*, **32**, 7537 (1999).
18. "Flow-Induced Crystallization of Polymers," G. Guerra and G. Titomanlio, Ed., Wiley-VCH, Verlag GmbH, 2002.
19. M. Hikosaka, S. K. Ghosh, and A. Toda, *Polym. Mater. Sci. Eng.*, **81**, 332 (1999).
20. S. Yamazaki, M. Hikosaka, A. Toda, I. Wataoka, and F. Gu, *Polymer*, **43**, 6585 (2002).
21. M. Tsuburaya and H. Saito, *Polymer*, **45**, 1027 (2004).
22. J. Koberstein, T. P. Russell, and R. S. Stein, *J. Polym. Sci., Polym. Phys. Ed.*, **17**, 1719 (1979).
23. R. S. Stein and P. R. Wilson, *J. Appl. Phys.*, **33**, 1914 (1963).
24. P. Debye and A. M. Bueche, *J. Appl. Phys.*, **20**, 518 (1949).
25. P. Debye, H. R. Anderson, Jr., and H. Brumberger, *J. Appl. Phys.*, **128**, 679 (1957).
26. R. S. Stein and S. N. Stidham, *J. Appl. Phys.*, **35**, 42 (1964).
27. Y. Koga and H. Saito, *Polymer*, **47**, 7564 (2006).
28. R. S. Stein and W. Chu, *J. Polym. Sci., Part A-2*, **8**, 1137 (1970).

